



INVITED ARTICLE

PELDOR in rotationally symmetric homo-oligomers

Angeliki Giannoulis^{a,b,c}, Richard Ward^{b,c}, Emma Branigan^b, James H. Naismith^b and Bela E. Bode^{a,b,c,*}

^a*EaStCHEM School of Chemistry, University of St Andrews, North Haugh, St Andrews, Fife, KY16 9ST, Scotland, UK;* ^b*Biomedical Sciences Research Complex, University of St Andrews, North Haugh, St Andrews, Fife, KY16 9ST, Scotland, UK;* ^c*Centre of Magnetic Resonance, University of St Andrews, North Haugh, St Andrews, Fife, KY16 9ST, Scotland, UK*

(Received 14 March 2013; final version received 12 April 2013)

Nanometre distance measurements by pulsed electron–electron double resonance (PELDOR) spectroscopy have become an increasingly important tool in structural biology. The theoretical underpinning of the experiment is well defined for systems containing two nitroxide spin-labels (spin pairs); however, recently experiments have been reported on homo-oligomeric membrane proteins consisting of up to eight spin-labelled monomers. We have explored the theory behind these systems by examining model systems based on multiple spins arranged in rotationally symmetric polygons. The results demonstrate that with a rising number of spins within the test molecule, increasingly strong distortions appear in distance distributions obtained from an analysis based on the simple spin pair approach. These distortions are significant over a range of system sizes and remain so even when random errors are introduced into the symmetry of the model. We present an alternative approach to the extraction of distances on such systems based on a minimisation that properly treats multi-spin correlations. We demonstrate the utility of this approach on a spin-labelled mutant of the heptameric Mechanosensitive Channel of Small Conductance of *E. coli*.

Keywords: DEER; pulsed dipolar spectroscopy; multiple spin effects; homo-oligomer; EPR

Introduction

Distance measurements by pulsed dipolar electron paramagnetic resonance (EPR) spectroscopy are a standard tool for generating distance constraints for structural modelling. The pulsed electron–electron double resonance (PELDOR or DEER for double electron–electron resonance) [1,2] method is increasingly applied to determine long-range distances [3,4]. Developments in commercial hardware, standardisation of pulse sequences [5] and readily accessible data analysis programs [6,7] have fuelled its widespread adoption.

A straightforward approach for using PELDOR is to covalently attach two nitroxide spin-labels (probes) to a macromolecule and measure the spin–spin distance. It is also possible to use singly labelled components of a system that forms oligomers. One of the major advantages of the method is that the probes are small (introduce limited perturbation) and since diamagnetic proteins are EPR silent, it allows the study of systems of tremendous size and complexity. The distance extraction is free from assumption about the system under investigation [6], thus unbiased structural constraints can be obtained. The characterisation of structural models for docking proteins or characterising a structural transition [8] by measuring a few well-chosen distances by PELDOR is very powerful [9]. Applications include synthetic model systems [5,10], soluble proteins

[11] and nucleic acids [12]. Recent advances have included membrane proteins [9], even though the local concentration of spins can pose a problem in phospholipid vesicle membranes [13,14] and care has to be taken when interpreting the data from detergent-solubilised samples [15]. In addition to the inter-spin distance, the number of coupled spin-labels [2,16], their relative orientation [17] and a potential exchange interaction [10,18] can be determined, yielding additional information. PELDOR has been applied on transient radicals [19], paramagnetic metal ions [20], spin-bearing clusters [21] and various possible pairs thereof [22].

PELDOR actually measures frequency modulations in the time domain and Tikhonov regularisation methods are commonly used to obtain the most appropriate distance distribution solution. This approach has been demonstrated to be reliable and robust [23] for spin pairs. The underpinning assumptions ignore some factors such as size-restriction effects [15] and effects caused by the presence of more than two spins in a molecule [24]. Other factors, including incomplete spin-labelling in multiply labelled samples and distributions of molecules not homogeneous in three dimensions [14] can introduce additional uncertainties in data analysis. An obvious concern is that if these factors are significant in an experiment, the derived distance distribution may be misleading.

*Corresponding author. Email: beb2@st-andrews.ac.uk

Here we focus on multi-spin effects in rotationally symmetric oligomeric membrane protein systems. These often have challenging spectroscopic parameters that hamper acquisition of high-quality data, especially in samples reconstituted into phospholipid vesicle membranes. Furthermore, the multi-spin effects present in oligomeric systems violate assumptions of the theory underlying the gold standard of data analysis: Tikhonov regularisation in the DEERAnalysis package [6], which uses a kernel function, explicitly written for a two-spin system (henceforth simply abbreviated TR). Thus, multi-spin systems are a special case formally beyond the scope of TR and, thus, the distance distributions generated should be used with caution. Approximating these systems as biradicals has given satisfactory results for the shortest distance present in the system (the vector from one molecule to its immediate neighbour) [25,26]. It has been shown [24] that multiply labelled systems will modulate with the product of the dipolar frequencies of all possible pairs. This leads to sum and difference frequencies that are currently ignored. A second feature that directly arises from the symmetry is correlations between distance vectors (in a rotationally symmetric system all vectors are mathematically related) that might enhance certain sum and difference frequencies while diminishing others. Even though PELDOR has been applied to homo-oligomers up to heptamers [26] and octamers [25] the only system in which these effects have been quantitatively considered is the tetrameric potassium channel KcsA [13]. However, the problem has been addressed in studies of the homo-trimeric sodium-coupled aspartate transporter [27]. Very recently, a promising approach for suppressing multiple spin artefacts by power-scaling the experimental data has been introduced and validated for up to five spins per molecule [28].

We now semi-quantitatively establish the significance of error introduced by the common practice of treating symmetric homo-oligomers as spin pairs. Secondly, we evaluate fitting experimental data using a reduced geometric model whilst retaining the multi-spin effects and symmetry correlations. Finally, we apply our new approach to data inversion with real data.

Multi-spin correlations in PELDOR

The underlying physical theory of PELDOR has been described in detail [2,3,29]. The following considerations focus entirely on rationalising the origin and theoretical treatment of multi-spin effects in systems bearing more than two spin labels. It is important to note that in all the following we assume the high-field, secular and point-dipole approximations to be valid and the electron–electron exchange interaction to be negligible. In addition, we approximate random mutual orientations between all possible pairs of spin-labels and thus diminish the effects of orientation selection for our simulated PELDOR data.

In a disordered powder sample the dipolar coupling between two spins will be determined by the spin–spin distance r and the angle θ between the distance vector and the external magnetic field:

$$\omega_{dd} = \frac{\mu_0 \mu_B^2 g_A g_B}{4\pi \hbar r^3} (1 - 3 \cos^2 \theta), \quad (1)$$

where g_A and g_B are the g values of the two coupled spins and are approximated to be isotropic, μ_0 is the vacuum permeability, μ_B is the Bohr magneton, \hbar is the Planck constant divided by 2π . The PELDOR signal $V(t)$ between two coupled spins can now be written straightforwardly as:

$$V(t) = V(0)(1 - \lambda[1 - \cos(\omega_{dd}t)]), \quad (2)$$

where λ is the fraction of B-spins inverted by the second frequency pulse. If we, furthermore, introduce powder averaging to take the random orientations of molecules in frozen solutions into account and consider the PELDOR signal of a system with more than two spins (i.e. n spins) as being the product of signals of the individual spin pairs we will arrive at the general form of the intra-molecular signal [16]:

$$V_{\text{intra}}(t) = \frac{V(0)}{n} \times \sum_{A=1}^n \int_0^{\pi/2} \prod_{\substack{B=1 \\ B \neq A}}^n \{1 - \lambda[1 - \cos(\omega_{dd}t)]\} \sin \theta d\theta. \quad (3)$$

The multiplication of dipolar frequencies in systems with more than two spins will lead to sum and difference frequencies, which in turn cause the dipolar spectrum to deviate from a superposition of Pake patterns [24]. This directly influences or even invalidates all data analysis approaches assuming the time domain signal to be a linear combination of spin pairs. An expansion of Equation (3) allows one to group the frequency contributions of the signal into pairs that oscillate with a single frequency and into triples, quadruples etc. that oscillate with a product of frequencies. While the absolute modulation depth Δ will contain pair and multi-spin contributions:

$$\Delta = 1 - (1 - \lambda)^{n-1}, \quad (4)$$

the coefficient of the pair contribution is described by [7]:

$$f_2 = \binom{n-1}{1} \lambda (1 - \lambda)^{n-2}, \quad (5)$$

where the first factor of the right-hand side of Equation (5) is the respective binomial coefficient. The k -spin contribution

oscillating with the product of $k - 1$ frequencies is given generally by:

$$f_k = \binom{n-1}{k-1} \lambda^{k-1} (1-\lambda)^{n-k}, \quad (6)$$

where the first factor of the right-hand side of Equation (6) is the respective binomial coefficient.

Each of those k -spin contributions will have a maximum at:

$$\lambda = \left(\frac{k-1}{n-1} \right). \quad (7)$$

Following Equation (7), the two-spin contribution will have a maximum at $\lambda = 1/(n-1)$. For a biradical this yields maximum two-spin contribution at $\lambda = 1$ while for an eightfold labelled system this maximum will be at $\lambda = 1/7$. Upon a further increase of λ the two-spin contribution will decrease. This implies that an upper limit of λ exists if data is to be analysed by TR [7]. It is important to note that Equation (6) implies that the ratio between the desired two-spin contribution and the unwanted multi-spin contributions will increasingly favour the former upon the reduction of λ (for details see supporting information). However, the reduction of λ will result in reduced dipolar modulation, thus for the rigorous use of TR a compromise must be reached between a reasonable modulation depth, to provide a good modulation-to-noise ratio, but suppressing significant contribution from the unwanted multi-spin effects. The choice of the smallest suitable λ for data analysis using TR is not trivial. Thus, one approach is to reduce the multi-spin correlations by a reduction of λ experimentally. This is currently under investigation and will be reported in due course. In contrast to the TR as implemented in DeerAnalysis, which ignores multi-spin effects, the use of a structural model allows one to explicitly forward calculate data under retention of product terms and mutual orientations of distance vectors. In the following section we describe such a model for homo-oligomers assuming rotational symmetry.

Definition of the model

In a reductionist approach we approximate the spin-label positions of quantitatively labelled, symmetric homo-oligomers of axis order n (n -mers) as being the vertex positions of the corresponding regular convex polygon (n -gon). Given the high symmetry of these systems (D_{nh}), all spin-spin distance vectors and their angular correlations are defined by n and the diameter (d) of the circle upon which the points sit. The inner angle α of the polygon is defined by Equation (8):

$$\alpha = \frac{n-2}{n} \pi. \quad (8)$$

In combination with d , Equation (8) uniquely defines the spin distances between all vertices:

$$r_{1i} = d \sin \frac{(i-1)(\pi-\alpha)}{2}, \quad (9)$$

with r_{1i} being the distance from the first vertex to the i th vertex.

In a polygon of even n a set of $n/2 - 1$ distances r_{1i} will be twofold degenerate while the longest distance (from position 1 to $i = n/2 + 1$) will be non-degenerate. In the case of odd n a set of $(n-1)/2$ distances r_{1i} will be twofold degenerate. Thus, only a total of $n/2$ or $(n-1)/2$ individual r_{1i} distances for even or odd n , respectively, need to be considered. Even though these well-defined distance ratios might be useful for restraining the distance distribution expected from the system under study [30], the implications of the model of regular convex n -gons go well beyond this. The orientations of the distance vectors and thus, their dipolar frequencies will be strongly correlated. All distance vectors will be lying in the plane of the polygon. In addition, n -gons with even n will have $n/2$ pairs of r_{12} -vectors being parallel in space and several other similarly obvious correlations can be constructed. Therefore, we chose here to explicitly calculate the vertex positions determining the distance vectors from those. This has the advantage of straightforward introduction of disorder into the model by simply displacing vertex positions. If, for convenience, we place the origin of the coordinate system on the symmetry axis within the plane of the n -gon and place the first vertex at the point $[0, d/2]$ the two-dimensional coordinates of the vertex positions for the n vertices (v_i) will be given by:

$$v_i = \left[\frac{d}{2} \sin((i-1)(\pi-\alpha)), \frac{d}{2} \cos((i-1)(\pi-\alpha)) \right]. \quad (10)$$

The only two parameters defining the spin-label positions in Equation (10) are n (via Equation (8)) and d . This allows the straightforward calculation of the PELDOR time trace according to Equation (3) retaining multi-spin effects and correlations between distance vectors.

Materials and methods

For the calculation of n -mers with n ranging from 3 to 8 the vertex positions have been calculated according to Equation (10) and displaced in a random direction in the polygon plane to achieve a Gaussian distribution of positions with a standard deviation σ that is given with the corresponding simulation. Corresponding to pulse excitations achievable in nitroxide-labelled samples at X-band frequencies, λ has been set between 0.4 and 0.5 unless explicitly stated otherwise and d between 3 and 9 nm have been tested. A low pass filter previously found to improve simulations has been used to treat the limited excitation of large dipolar

couplings during data fitting [31]. To avoid $(n - 1)$ nested loops necessary for the calculation of the powder average of the polygon time trace via Equation (3), we have chosen to perform Monte Carlo simulations allowing n random vertex displacements and a random orientation of the magnetic field vector in each trial. For simulations each time trace consists of 10,000 Monte Carlo trials while for fitting procedures 5000 trials were found to yield sufficient results for n up to 8. During all simulations the individual distances of the model were used for generating a ‘true’ distance distribution. From this ‘true’ distance distribution a second time trace has been calculated which deliberately neglects all multi-spin correlations for representation of the hypothetical case of irrelevant multi-spin effects. This latter trace has been scaled to match the modulation depth Δ of the originally simulated time trace. Visual inspection of the time trace, including multi-spin correlations and the artificial pair contribution trace already gives an estimate of the magnitude of deviations that is confirmed by calculating the RMSD (root mean square deviation) between distance distributions by TR and the ‘true’ distribution. All simulations have been performed assuming quantitative spin labelling. All time traces underwent TR in DeerAnalysis2011 with the regularisation parameter chosen by the L-curve criterion. All distance distributions have been normalised on maximum intensity.

Selected simulations and experimental PELDOR time traces obtained on a spin labelled mutant (S147C) of the Mechanosensitive Ion Channel of Small Conductance (MscS) of *E. coli* have been fitted by constructing the vertex positions according to Equation (10) and minimising the deviation between simulation and experiment (note that experiment in the first case means Monte Carlo simulation of a regular convex polygon). Experimental data on MscS has been reported [26] and fitted in DeerAnalysis2011 [6]. We refit the data with retention of the modulation depth information and parameters n , σ , λ , d applying the low-pass filter. We assume 100% efficiency of labelling where the multi-spin effects are most pronounced as the problem approximately scales with λ times labelling efficiency. The model function is available from the authors upon request.

Results and discussion

A diameter of 5 nm was chosen for initial simulations and vertices were displaced to yield a standard deviation of 0.1 nm in the polygon plane. From these coordinates the time traces have been calculated according to Equation (3) (denoted ‘multi-spin’ trace). The actual distance distribution arising from these coordinates was calculated in real space (denoted ‘true’ distribution). From this distance distribution a second time trace has been calculated neglecting all multi-spin terms of Equation (3) prior to rescaling to meet the modulation depth governed by Equation (4) (denoted as ‘spin pairs’). Thus, the ‘multi-spin’ trace

contains all effects caused by the presence of multiple spins in one molecule, while the ‘spin pairs’ trace has them eliminated. The ‘spin pairs’ trace is valid for analysis by TR and all deviations between distance distributions generated from the ‘spin pairs’ and the ‘multi-spin’ time traces are entirely due to multi-spin effects. The initial exploration of the time domain traces is depicted in Figure 1. An increasing loss of visible modulation in the ‘multi-spin’ traces as compared to the ‘spin pairs’ traces becomes evident when increasing n from equilateral triangle to octagon. While the ‘multi-spin’ modulation merely seems damped for the triangle and square, low frequencies appear to vanish from the pentagon onwards. In the case of the octagon only a hump very early in the time trace is left while all other frequencies have been damped, nicely illustrating the extreme impact that multi-spin effects can have on the data analysis.

These qualitative findings are quantitatively confirmed when the data is inverted to the distance domain. We have subjected both ‘multi-spin’ and ‘spin pair’ traces to TR in DeerAnalysis to generate distance distributions that were superimposed with the ‘true’ distributions and the respective RMSD is given in Table 1.

The trend clearly shows that the deviations between ‘true’ and ‘spin pair’ only moderately increase with n . Those between the ‘true’ and the ‘multi-spin’ distributions are already worse for the triangle and increase even more severely with n . This behaviour is also found by visual inspection (Figure 1). While the triangular ‘multi-spin’ simulations yield a set of low amplitude distance peaks which seem to be easily assigned artefacts or ‘ghost peaks’ from data processing, the square and pentagon already display excessively broadened r_{12} distance peaks while r_{13} is diminished in amplitude. From hexagon to octagon the shortest distance obtained from the ‘multi-spin’ simulation is significantly broadened and its mean at times slightly shifted while all other distances are diminished so far that they cannot be recovered from the artefact peaks unequivocally. The data inversion on the ‘spin pairs’ time traces reproduces the ‘true’ distributions highly accurately. We attribute this to the fact that we have created a best-case scenario for TR. The main experimental uncertainties of thermal noise

Table 1. RMSD between ‘true’ distance distributions and those by TR.

Polygon	RMSD between ‘spin pair’ and ‘true’ distributions	RMSD between ‘multi-spin’ and ‘true’ distributions
Triangle	0.0432	0.0628
Square	0.0380	0.0928
Pentagon	0.0671	0.1672
Hexagon	0.0781	0.1833
Heptagon	0.0625	0.2037
Octagon	0.0776	0.2083

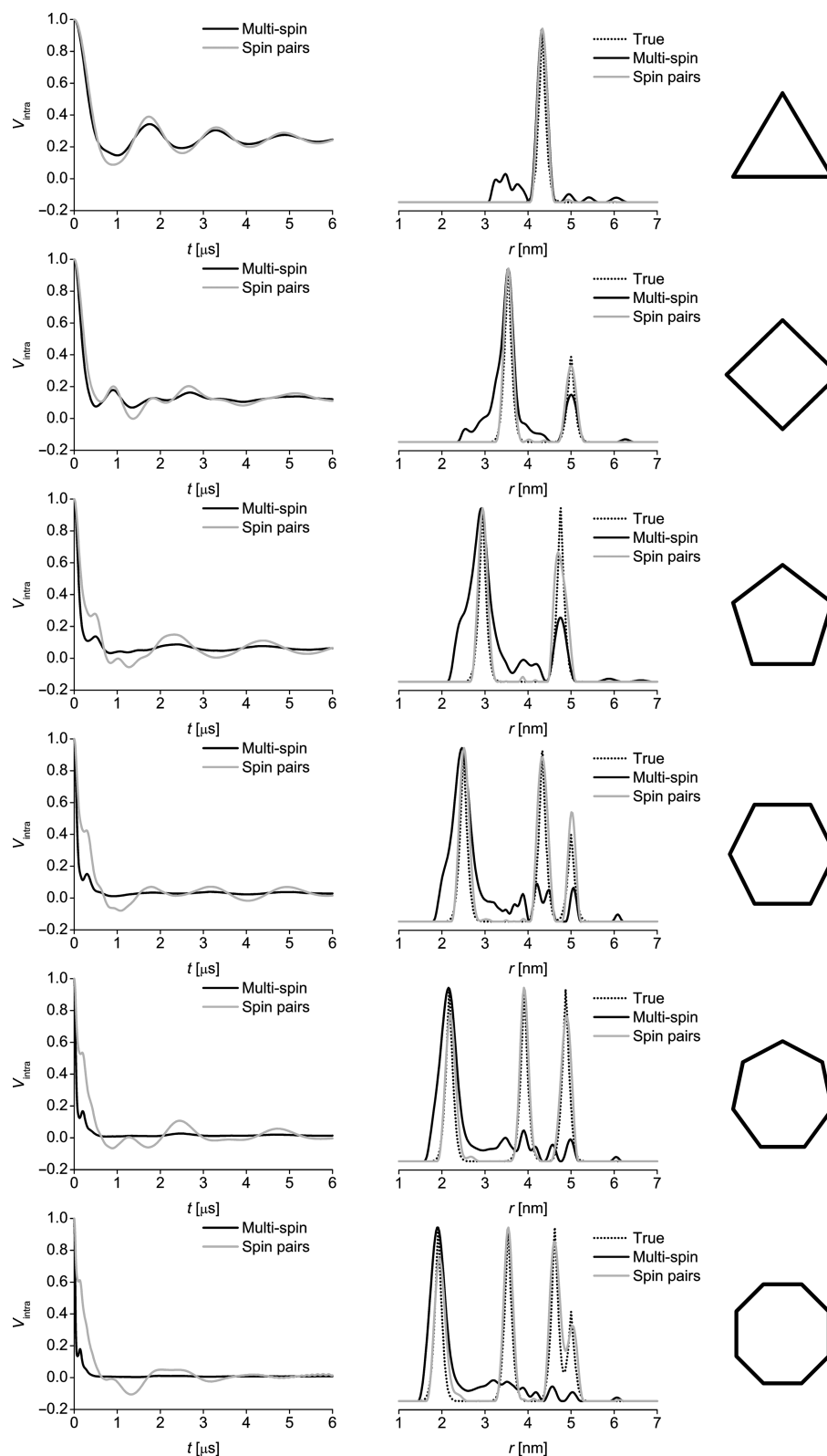


Figure 1. Simulations of symmetric multi-spin systems arranged as regular convex polygon from triangle to octagon with the polygon type depicted to the right. The time domain data are depicted to the left. Black traces explicitly treat all coupled spins via product formation, whereas grey traces are calculated neglecting multi-spin effects exclusively assuming spin pairs. Distance domain data is shown to the right of the respective time trace; the 'true' spin-spin distance distribution resulting from polygon type and vertex displacement is depicted as black dotted lines. Distance domain data by TR are depicted in black and grey in accordance with the respective time traces. All polygon diameters (d) are 5 nm. Vertices are displaced in plane with a standard deviation (σ) of 0.1 nm. The probability of exciting a coupled spin (λ) is 0.5.

and background correction are absent from this data, as are errors arising from the truncation of time domain data (simulated data has a length of $6 \mu\text{s}$ allowing us to observe a full modulation for distances of slightly over 6 nm). This emphasises even more the severity of the distortions of distance distributions obtained without due consideration of multi-spin effects.

We have explored the influence of the size of the circumference for different orders of rotational symmetry. To resemble feasible experimental parameters we chose $\lambda = 0.4$ (instead of $\lambda = 0.5$ for the initial exploration in Figure 1) for all following simulations and truncated the time traces at $5 \mu\text{s}$ length. A lower limit on diameters d of 4 nm occurs because smaller polygons give rise to very short vectors (particularly for higher-order rotational axis) beyond the scope of PELDOR.

Diameters above 7 nm lead to significant truncation of dipolar modulations. Within these limits, we observe excellent agreement with data in Figure 1, while smaller and larger polygons ($d < 4 \text{ nm}$ and $d > 7 \text{ nm}$, respectively) agree qualitatively (see supporting information). We suggest that the preservation of our central observation on the effect of multiple spins has eliminated polygon size, symmetry order or an unreasonably high λ as possible causes of the distortion. Thus, the question arises whether the broadening of the shortest distance is significant in systems that already exhibit significantly broader distance peaks caused by structural heterogeneity. We constructed tests of different symmetry ($n = 3$ to 8) and a fixed diameter of 6 nm but with the vertices displaced randomly by standard deviations of 2%, 5% and 10% of the diameter (i.e. 0.12, 0.3 and 0.6 nm).

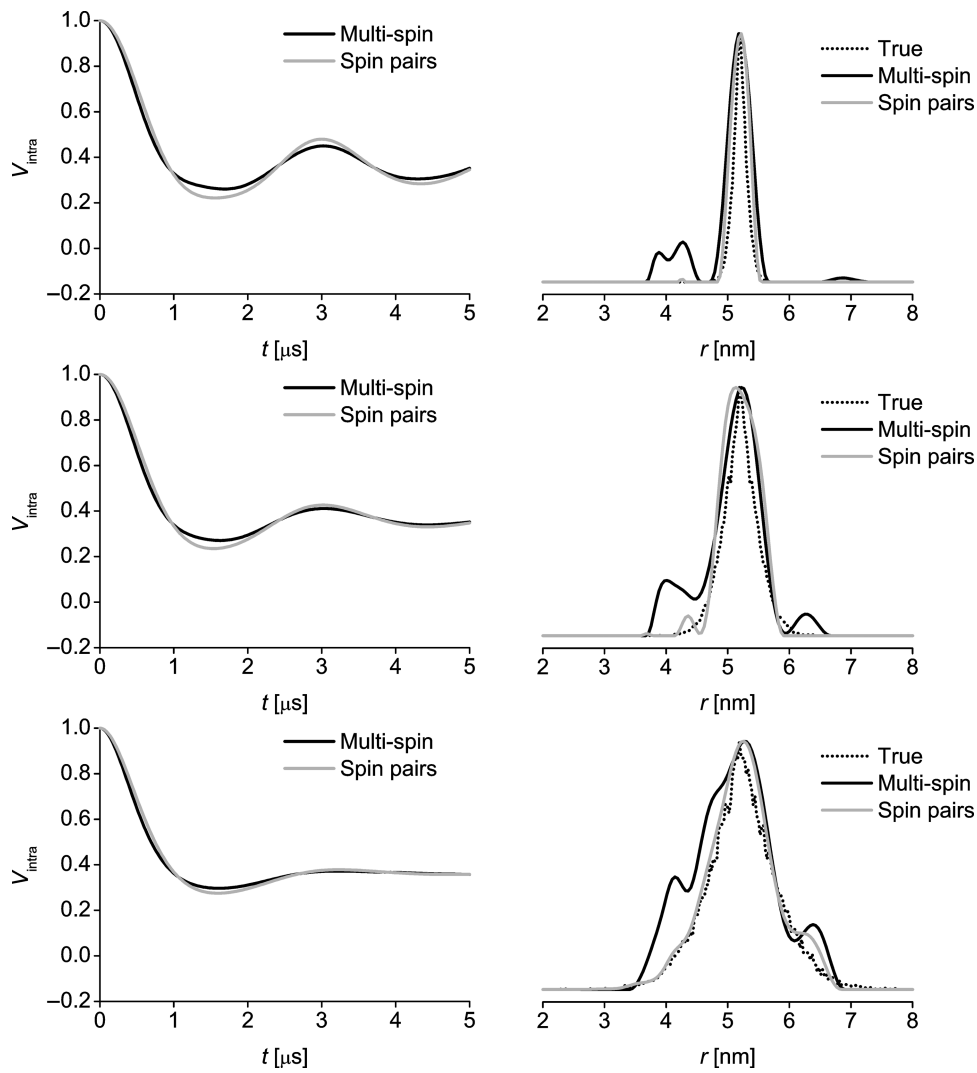


Figure 2. Simulations of different vertex displacements in a triangular model of $d = 6 \text{ nm}$. Standard deviation of vertex displacement is (from top to bottom) 0.12, 0.3 and 0.6 nm, $\lambda = 0.4$, otherwise colours and order of panels is similar to Figure 1.

Figure 2 demonstrates that for the range of heterogeneities tested the multi-spin effects lead in all cases to detectable broadening of the distance distributions. Monte Carlo noise present in the ‘true’ distribution with the largest vertex displacement has no impact on the quantitative results. The time domain data reveals that intrinsic broad distance distributions suffer less from these artefacts. However, in trying to extract the highest quality distance distributions, these results indicate that broadening by multi-spin effects cannot be neglected even in the presence of broad intrinsic distributions.

Figure 3 displays the effects of symmetry imperfection for a heptagon model. At increasing displacements the distance distributions obtained from the ‘spin pair’ time trace increasingly deviate from the ‘true’ distance distribution. This is tentatively attributed to the less pronounced mod-

ulation in the time trace in addition to slight truncation of dipolar modulations. It can be seen that the medium distance peak in these distributions splits and that the long distance peak is artificially narrowed, while the ratio of the integral distance peaks appears to remain constant. This seems to indicate per se limitations of TR of complex distance distributions and is currently under investigation. However, even considering the emerging disagreement between ‘spin pair’ and ‘true’ distributions the deviations of the ‘multi-spin’ distance distributions remain much more severe. In addition to substantial broadening of the short distance peak, the longer distances have lost most of their intensity making these distributions very unreliable to interpret.

These results clearly show that neglect of multi-spin effects leads to considerable distortion of distance distributions, especially in systems exceeding four spins. This

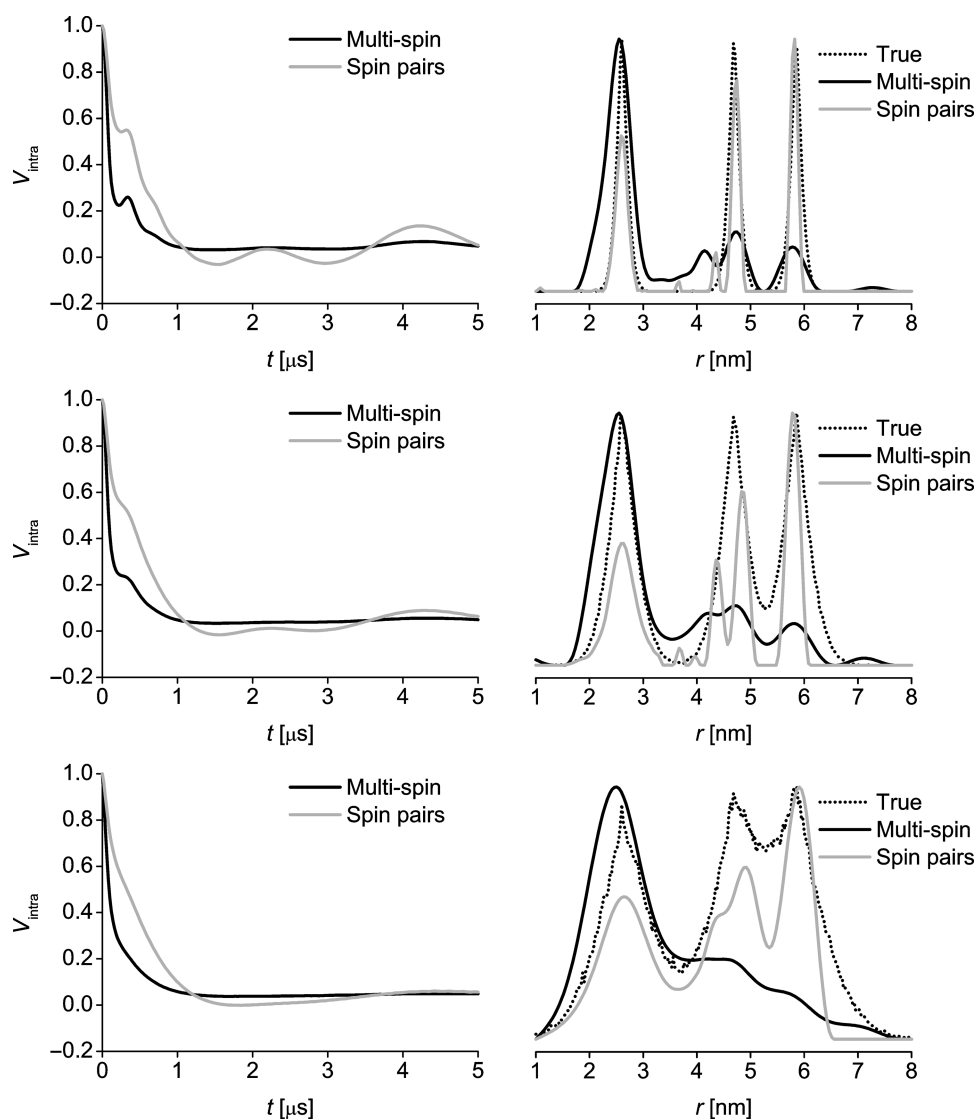


Figure 3. Simulations of different vertex displacements in a heptagon system. For all other details see Figure 2.

makes analysis of longer distances especially those originating from higher-order vectors (r_{13} , r_{14} etc.) difficult. The potential for erroneous interpretation is high. Some existing studies have focused only on the shorter r_{12} vectors, which are much less sensitive to these problems, but at the cost of throwing away information contained in the data [25, 26].

Fitting of a model polygon

In an alternative approach to data analysis we have chosen to explicitly forward calculate our data based on the polygon model and to extract structural parameters by minimisation of the deviation between simulation and experiment. Several initial tests have shown that the simultaneous fitting of several parameters was less stable, especially with increasing n . From the behaviour of the fit routine we detect multiple local minima, while the dampening of modulation in ‘multi-spin’ simulations of heptagons and octagons suggests a very shallow global minimum. Thus, we chose to approach the minimisation from initial simulations for achieving reasonable agreement by visual inspection and optimising d and σ iteratively or simultaneously from this

starting point. As the function is defined by n , d , σ , λ , labelling degree and the low-pass filter for suppression of large dipolar frequencies, we emphasise here, that only the optimisations of d and σ have been tested. All other parameters are accessible from different experiments or assumptions and their optimisation is beyond the scope of this approach (attempts to minimise by calculation results in severely under-determined functions).

In an initial test of the feasibility of the approach we have taken simulated data on an octagon with $d = 6$ nm, $\lambda = 0.4$ and varying standard deviation of vertex displacement of 0.12, 0.3 and 0.6 nm. The ‘multi-spin’ traces of these simulations are fitted to the same mathematical model they were initially simulated with (although good agreement between the ‘true’ distribution and its fit is expected it validates the approach).

Best fit results in Figure 4 have been obtained by least square fitting of d and σ . Monte Carlo noise visible in ‘true’ and ‘fit’ distance distributions of larger σ have been found not to affect the fit stability, but can be reduced for cosmetic reasons by increasing the number of Monte Carlo trials. In all three cases the agreement of ‘true’ distribution and its fit by far surpasses the quality of TR as judged by the eye.

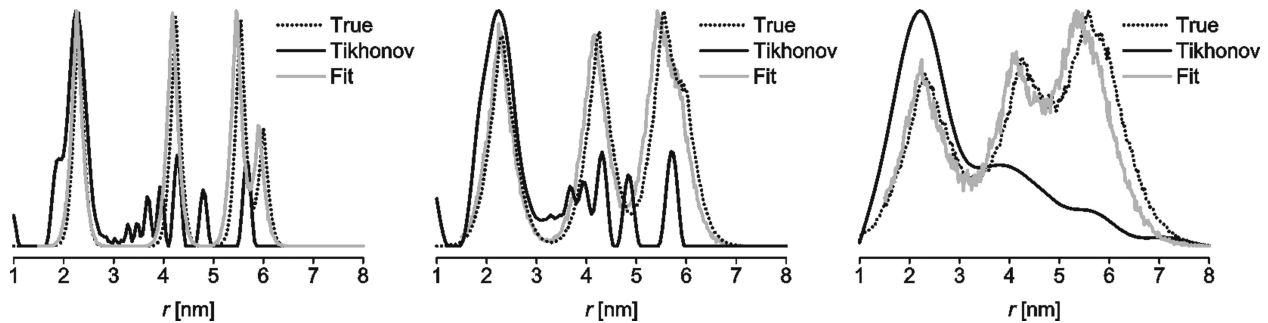


Figure 4. Analysis of simulated data of an octagon with $d = 6$ nm, $\lambda = 0.4$ and varying standard deviation of vertex displacement of 0.12 (left), 0.3 (middle) and 0.6 nm (right). ‘True’ distance distribution in black dots, ‘fit’ in light grey and ‘multi-spin’ TR in black solid lines (for details see the main text).

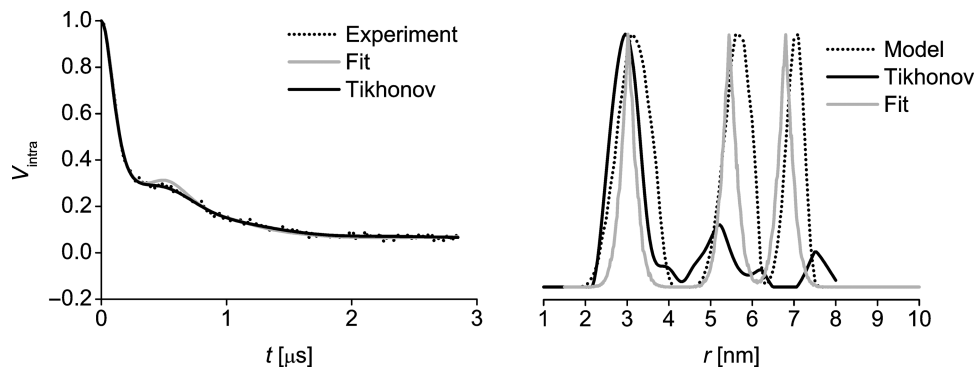


Figure 5. Analysis of the spin-labelled S147C mutant of MscS. Time domain data is depicted in the left panel; experimental data is given in as black dotted line, time trace based on TR as black solid line and time trace based on fit results as grey solid line. The distance domain data is shown to the right. Results from TR are given as black solid line, distance distribution from heptagon fit as grey solid line and modelling based on the crystal structure as black dotted line.

Interestingly all three fits slightly underestimate d that we attribute to the effects of the truncation of the time trace which would under-penalise deviations in low frequencies caused by long distances and to the use of the low-pass filter suppressing of large dipolar frequencies during the fit.

For further demonstration of the usefulness of this approach we have subjected data obtained on a spin-labelled mutant (S147C) of the MscS of *E. coli* [26] to this fitting procedure assuming the heptameric protein to have heptagonal symmetry. The results in Figure 5 demonstrate a slightly worse agreement between time traces from the minimised heptagon model and the experiment compared to the time trace from TR. If, however, the distance domain data is examined the value of this new approach becomes evident immediately. Even though we find a slight underestimation of the polygon diameter, as before, the distance distribution obtained by fitting a polygon model is by far closer to the rotamer model based on the crystal structure [32] than the distance distribution obtained by TR, which neglects multi-spin correlations. An increased reliability in the extraction of multiple distances of rotationally symmetric homo-oligomers may prove valuable to identify multiple functional states present or to characterise structural flexibility. Thus, we are convinced we have satisfactorily demonstrated the need and feasibility of alternative data analysis approaches for PELDOR measurements in spin-labelled homo-oligomers.

Conclusion

In PELDOR measurements on systems with more than two spins multi-spin correlations arise that can hamper data analysis. For symmetric homo-oligomeric systems that can be approximated by regular convex polygons this results in a broadening of the distance distribution, an occasional shifting of distance peaks and a substantial loss of intensity of the distance peaks of all but the shortest distance. Simulations neglecting multi-spin correlations can introduce error. The approach of forward calculation of PELDOR data yields consistently superior results for model systems. Crucially, and in contrast to the established methods, this new approach allows reliable extraction of all three non-degenerate distances from experimental data on a heptameric membrane protein.

Acknowledgements

We thank Prof. Gunnar Jeschke for implementing the retention of modulation depth information during model fitting in DeerAnalysis and Prof. Olav Schiemann for helpful discussions on PELDOR of MscS. AG is grateful for a postgraduate fellowship by the EPSRC-funded doctoral training centre 'integrated magnetic resonance'. BEB is currently supported by an EaStCHEM Hirst Academic Fellowship by the School of Chemistry, St Andrews and funding from the People Programme (Marie Curie Actions) of the European Union's Seventh Framework Pro-

gramme (REA 334496). JHN acknowledges BBSRC support (BB/H017917/1) and Wellcome Trust support (WT092552MA).

References

- [1] A.D. Milov, K.M. Salikov, and M.D. Shirov, *Fiz. Tverd. Tela* **23**, 975 (1981).
- [2] A.D. Milov, A.B. Ponomarev, and Y.D. Tsvetkov, *Chem. Phys. Lett.* **110**, 67 (1984).
- [3] G. Jeschke and Y. Polyhach, *Phys. Chem. Chem. Phys.* **9**, 1895 (2007); O. Schiemann and T.F. Prisner, *Quart. Rev. Biophys.* **40**, 1 (2007).
- [4] G. Jeschke, *Annu. Rev. Phys. Chem.* **63**, 419 (2012).
- [5] M. Pannier, S. Veit, A. Godt, G. Jeschke, and H.W. Spiess, *J. Magn. Reson.* **142**, 331 (2000).
- [6] G. Jeschke, V. Chechik, P. Ionita, A. Godt, H. Zimmermann, J. Banham, C.R. Timmel, D. Hilger, and H. Jung, *Appl. Magn. Reson.* **30**, 473 (2006).
- [7] G. Jeschke, in *Structure & Bonding* (in press), doi: 10.1007/430_2011_61 (Springer, Berlin, 2012).
- [8] G. Jeschke, *J. Chem. Theory Comput.* **8**, 3854 (2012).
- [9] C. Altenbach, A.K. Kusnetzow, O.P. Ernst, K.P. Hofmann, and W.L. Hubbell, *Proc. Natl. Acad. Sci. USA* **105**, 7439 (2008).
- [10] A. Weber, O. Schiemann, B. Bode, and T.F. Prisner, *J. Magn. Reson.* **157**, 277 (2002).
- [11] Z. Zhou, S.C. DeSensi, R.A. Stein, S. Brandon, M. Dixit, E.J. McArdle, E.M. Warren, H.K. Kroh, L. Song, C.E. Cobb, E.J. Hustedt, and A.E. Beth, *Biochemistry* **44**, 15115 (2005); J.E. Banham, C.R. Timmel, R.J.M. Abbott, S.M. Lea, and G. Jeschke, *Angew. Chem. Int. Ed.* **45**, 1058 (2006); G.W. Reginsson and O. Schiemann, *Biochem. Soc. Trans.* **39**, 128 (2011).
- [12] O. Schiemann, A. Weber, T.E. Edwards, T.F. Prisner, and S.T. Sigurdsson, *J. Am. Chem. Soc.* **125**, 3434 (2003); O. Schiemann, N. Piton, Y. Mu, G. Stock, J.W. Engels, and T.F. Prisner, *J. Am. Chem. Soc.* **126**, 5722 (2004); A. Marko, V. Denysenkov, D. Margraf, P. Cekan, O. Schiemann, S.T. Sigurdsson, and T.F. Prisner, *J. Am. Chem. Soc.* **133**, 13375 (2011).
- [13] B. Endeward, J.A. Butterwick, R. MacKinnon, and T.F. Prisner, *J. Am. Chem. Soc.* **131**, 15246 (2009).
- [14] R. Dastvan, B.E. Bode, M.P.R. Karuppiah, A. Marko, S. Lyubenova, H. Schwalbe, and T.F. Prisner, *J. Phys. Chem. B* **114**, 13507 (2010).
- [15] B.E. Bode, R. Dastvan, and T.F. Prisner, *J. Magn. Reson.* **211**, 11 (2011).
- [16] B.E. Bode, D. Margraf, J. Plackmeyer, G. Dürner, T.F. Prisner, and O. Schiemann, *J. Am. Chem. Soc.* **129**, 6736 (2007).
- [17] R.G. Larsen and D.J. Singel, *J. Chem. Phys.* **98**, 5134 (1993); O. Schiemann, P. Cekan, D. Margraf, T.F. Prisner, and S.T. Sigurdsson, *Angew. Chem., Int. Edit.* **48**, 3292 (2009).
- [18] D. Margraf, P. Cekan, T.F. Prisner, S.T. Sigurdsson, and O. Schiemann, *Phys. Chem. Chem. Phys.* **11**, 6708 (2009).
- [19] M. Bennati, A. Weber, J. Antonic, D.L. Perlstein, J. Robblee, and J. Stubbe, *J. Am. Chem. Soc.* 14988 (2003); A. Savitsky, A.A. Dubinskii, M. Flores, W. Lubitz, and K. Möbius, *J. Phys. Chem. B* **111**, 6245 (2007).
- [20] I.M.C.v. Amsterdam, M. Ubbink, G.W. Canters, and M. Huber, *Angew. Chem. Int. Ed.* **42**, 62 (2003); S. Pornsuwan, C.E. Schafmeister, and S. Saxena, *J. Phys. Chem. C* **112**, 1377 (2008).
- [21] M.M. Roessler, M.S. King, A.J. Robinson, F.A. Armstrong, J. Harmer, and J. Hirst, *Proc. Natl. Acad. Sci. USA* **107**, 1930 (2010).

- [22] C. Elsässer, M. Brecht, and R. Bittl, *J. Am. Chem. Soc.* **124**, 12606 (2002); E. Narr, A. Godt, and G. Jeschke, *Angew. Chem. Int. Ed.* **41**, 3907 (2002); I.V. Borovykh, S. Ceola, P. Gajula, P. Gast, H.-J. Steinhoff, and M. Huber, *J. Magn. Reson.* **180**, 178 (2006).
- [23] G. Jeschke, G. Panek, A. Godt, A. Bender, and H. Paulsen, *Appl. Magn. Reson.* **26**, 223 (2004); Y.-W. Chiang, P.P. Borbat, and J.H. Freed, *J. Magn. Reson.* **172**, 279 (2005).
- [24] G. Jeschke, M. Sajid, M. Schulte, and A. Godt, *Phys. Chem. Chem. Phys.* **11**, 6580 (2009).
- [25] G. Hagelueken, W.J. Ingledew, H. Huang, B. Petrovic-Stojanovska, C. Whitfield, H. Elmami, O. Schiemann, and J.H. Naismith, *Angew. Chem., Int. Ed.* **48**, 2904 (2009).
- [26] C. Pliotas, R. Ward, E. Branigan, A. Rasmussen, G. Hagelueken, H. Huang, S.S. Black, I.R. Booth, O. Schiemann, and J.H. Naismith, *Proc. Natl. Acad. Sci. USA* **109**, 15983 (2012).
- [27] E.R. Georgieva, P.P. Borbat, C. Ginter, J.H. Freed, and O. Boudker, *Nat. Struct. Mol. Biol.* **20**, 215 (2013).
- [28] T. von Hagens, Y. Polyhach, M. Sajid, A. Godt, and G. Jeschke, *Phys. Chem. Chem. Phys.* **15**, 5854 (2013).
- [29] A.D. Milov, A.G. Maryasov, and Y.D. Tsvetkov, *Appl. Magn. Reson.* **15**, 107 (1998).
- [30] O. Dalmas, H.C. Hyde, R.E. Hulse, and E. Perozo, *J. Am. Chem. Soc.* **134**, 16360 (2012).
- [31] B.E. Bode, J. Plackmeyer, T.F. Prisner, and O. Schiemann, *J. Phys. Chem. A* **112**, 5064 (2008).
- [32] G. Hagelueken, R. Ward, J. Naismith, and O. Schiemann, *Appl. Magn. Reson.* **42**, 377 (2012).